Proceedings of the ASME 2016 International Mechanical Engineering Congress & Exposition
ASME 2016 IMECE
November 11-17, 2016, Phoenix, Arizona, USA

IMECE2016-66809

PARAMETER ESTIMATION FOR HVAC SYSTEM MODELS FROM STANDARD TEST DATA

Hannah Luthman
Graduate Research Engineer, Boise State University
Boise, Idaho, USA

Dr. John F. Gardner
Professor of Mechanical & Biomechanical Engineering, Boise State University
Boise, Idaho, USA

ABSTRACT

Nearly all cooling systems, and an increasing proportion of heating systems, utilize the vapor compression cycle (VCC) to provide and remove heat from conditioned spaces. Even though the application of VCC's throughout the built environment is ubiquitous, effective and accessible models of the performance of these systems remains elusive. Such models could be important tools for equipment and building designers, and building energy managers and those who are attempting to optimize building energy performance through the use of model-based control systems. A quasi-steady state, spreadsheet-based model has been developed which requires knowledge of 10 system-specific parameters. A method utilizing manufacturer's test conditions to derive these values is presented.

The model is applied to three commercially available units and a subset of test conditions is used to identify the model parameters. The model is validated over the entire range of conditions with modeling errors ranging from 2 to 4%.

INTRODUCTION

Commercial and residential buildings account for a large portion of society's energy consumption. Of that usage, space conditioning is a significant component. Yet, in spite of the widespread use of air conditioning systems, the ability to predict performance in off-design conditions is limited.

The vapor compression cycle (VCC) is predominately used to remove heat from (and sometimes provide heat to) conditioned space by use of a circulating refrigerant [1]. In cooling systems, this refrigerant is used to transfer heat from the air inside the conditioned space to the outside environment. Advances have been made in the design and operation of these mechanical refrigeration systems, yet, in order to increase the operating efficiency of these units, the ability to model their performance must also evolve.

Traditional modeling of VCC units is largely empirical in nature and performance under different conditions amounts to finding the load points at intersections of component performance curves [2]. Many attempts at computer-based predictive models were attempts to mimic this process [3] [4].

More recently, motivated by the promise of high performance model-based control approaches, researchers have developed fundamental, physics based dynamic models exemplified by the groundbreaking work by He [5]. This work has been expanded by others such as Alleyne and Li [6]. These approaches utilize a moving boundary method to capture the complexities of the heat transfer in the evaporator and condenser as the boundaries between single phase and two-phase flow move under various operating conditions.

PREVIOUS MODLEING EFFORTS

As opposed to approaches using multiple fixed-length lumps to model heat exchangers, the moving boundary method utilizes a minimum number of variable length control volumes, the length of which changes as operating conditions change, capturing what occurs in the actual devices. The dynamic model generated by He[5] is developed for a cross-flow type heat exchanger with R-22 refrigerant filled tubing and air as the secondary fluid. The heat transferred from the refrigerant to the tube wall as well as the tube wall to the atmosphere are both considered. The matrix of equations presented by He for both the evaporator and the condenser encompasses both energy balance equations as well as mass balance equations due to the nature of the partial derivatives [5]. His study focuses on the dynamic performance of a VCC unit that is under changing operating conditions. Since then, McKinley and Alleyne have published research to address concerns with He's research regarding heat exchanger design, non-uniform air temperature

distribution as well as non-circular refrigerant passages [7]. Their work supports the moving boundary method over a finite volume model but notes the probability of the model becoming singular and failing under atypical operation. This operation includes the possibility lengths of some of the zones could go to zero and hence the number of zones within the heat exchangers can be variable and not fixed. Later, working with Alleyne & Li took the research a step further to understand the basis of operation when the VCC unit starts and stops [6]. It is during this start-up and stopping operation that one will see majority of the differing number of zones.

REFRIGERATION CYCLE MODELING

Thermodynamic States

To define the thermodynamic states used in the analysis, a review of the cycle is presented. Figure 1 shows the T-S diagram for a typical VCC including superheat and sub cool in the evaporator and condenser, respectively.
The analysis laid out in this paper utilizes a realistic VCC system with reference to the states as shown in Figure 1. These states and their refrigerant properties at each zone are shown in Table 1.

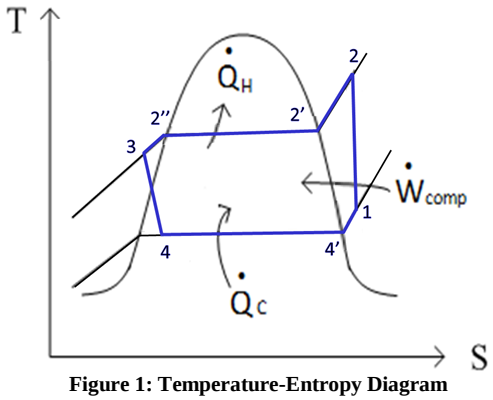

Figure 1: Temperature-Entropy Diagram of the VCC showing condenser sub-cool and evaporator superheat.

Assumptions

The assumptions underlying the modeling effort are:

- No pressure drop across heat exchangers
- No temperature change between State 4 and State 4'
- No temperature change between State 2' and State 2''
- Consistent ambient air temperature across the condenser
- Uniform void fraction
- 85% Isentropic compressor efficiency
- Negligible refrigerant mass in the compressor, flow restrictor, and additional tubing
- Proper system charge
- Information from manufacturer was detailed and accurate

Table 1: Thermodynamic States of a VCC System

State	Refrigerant Phase
1	Refrigerant leaves evaporator as a superheated vapor and enters the compressor
2	Refrigerant leaves compressor as a superheated vapor with increased pressure and enters the condenser
cr1	Average state values in first condenser region; between State 2 and State 2'
2'	Refrigerant within condenser phase changes from superheated vapor to saturated vapor then a liquid / vapor two-phase combination
2''	Refrigerant within condenser phase changes from a liquid / vapor two-phase combination to a saturated liquid
cr3	Average state values in third condenser region; between State 2' and State 2''
3	Refrigerant leaves the condenser as a subcooled liquid and enters the flow restrictor
4	Refrigerant leaves the flow restrictor as a liquid / vapor two-phase combination and enters the evaporator with a reduced pressure
4'	Refrigerant within the evaporator phase changes from a liquid / vapor two-phase combination to a saturated vapor
er2	Average state values in second evaporator region; between State 4' and State 1

MOVING BOUNDARY METHOD

While the compressor and flow constrictor (e.g. the thermal expansion valve) of refrigeration systems are often to focus of analysis, the majority of system operation happens within the heat exchangers (evaporator and condenser) of the system. As previously discussed, the moving boundary method, while more complicated in development, offers a more efficient model due to the fact that it utilizes only 2 to 3 control volumes in each heat exchanger. Previous researchers have found that fixed-lump approaches lead to simulations that a factor of two to four times slower than a simulation using the moving boundary model [8] [7].

There are three sectors within the condenser, superheated vapor, saturated mixture and the subcooled liquid as seen in Figure 2. For the evaporator there are two sectors, the two-phase mixture and the superheated vapor as seen in Figure 3. The lengths of these zones are variable depending on operating conditions. This differs from the fixed length zone models that has the heat exchangers broken up into multiple zones with unchanging lengths. The use of the minimal number of zones significantly reduces the calculations required to track the

refrigerant's thermodynamic state during its flow through the heat exchangers yet it still provides an accurate overall analysis.

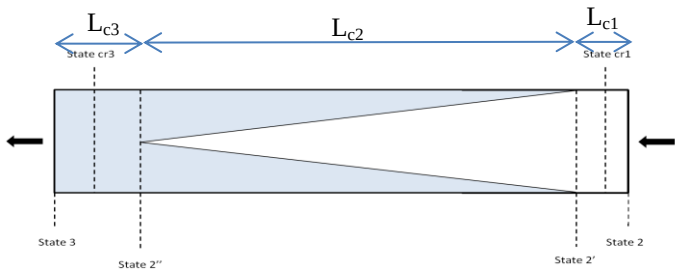

Figure 2: Conceptual model of the condenser, showing superheat, saturation and subcooled regions.

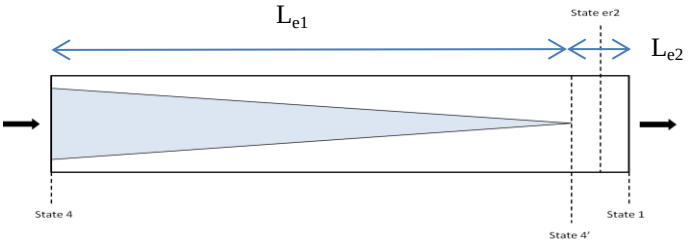

Figure 3: Conceptual model of the evaporator, showing saturated and superheat regions.

A key simplification used is the assumption that there is no pressure drop across either of the heat exchangers, an assumption typically applied to these devices, supported by the fact that refrigerant flow rates and velocities are rather modest by design [9].

Evaporator Dynamic Equations

The goal of this study is a spread-sheet based model to predict steady state performance for various outside and inside air temperatures. The process begins with the moving boundary dynamic model from the literature because those are better developed models and the we wish to incorporate the moving boundary feature in our models. Starting with the dynamic state equations found in [5], the evaporator dynamics are described using 5 state equations and shown in Equation (1).

$$\boldsymbol{D}_E \dot{x}_E = f_E(x_E, u_E) \qquad (1)$$

where the dynamic states are:

$$x_E = [L_{e1}\ P_E\ h_{eo}\ T_{ew1}\ T_{ew2}]^T$$

and the inputs are:

$$u_E = [\dot{m}_1\ h_1\ \dot{m}_2\ v_E]^T$$

$$f_E = \begin{bmatrix} \dot{m}_i h_i - \dot{m}_i h_g + \alpha_{i1}\pi D_i L_1 (T_{w1} - T_{r1}) \\ \dot{m}_o h_g - \dot{m}_o h_o + \alpha_{i2}\pi D_i L_2 (T_{w2} - T_{r2}) \\ \dot{m}_i - \dot{m}_o \\ \alpha_{i1}\pi D_i (T_{r1} - T_{w1}) + \alpha_o \pi D_o (T_a - T_{w1}) \\ \alpha_{i2}\pi D_i (T_{r2} - T_{w2}) + \alpha_o \pi D_o (T_a - T_{w2}) \end{bmatrix}$$

and $\mathbf{D}_E$ is a matrix expressing the coupled nature of the state equations as detailed in [5].

Condenser Dynamic Equations

Similarly, Equation (2) describes the condenser dynamics using 7 state equations.

$$\boldsymbol{D}_C \dot{x}_C = f_C(x_C, u_C) \qquad (2)$$

where the dynamic states are:

$$x_C = [L_{c1}\ L_{c2}\ P_C\ h_{co}\ T_{cw1}\ T_{cw2}\ T_{cw3}]^T$$

and the inputs are:

$$u_C = [\dot{m}_2\ h_3\ \dot{m}_1\ v_C]^T$$

$$f_C = \begin{bmatrix} \dot{m}_i h_i - \dot{m}_i h_g + \alpha_{i1}\pi D_i L_1 (T_{w1} - T_{r1}) \\ \dot{m}_o h_g - \dot{m}_o h_l + \alpha_{i2}\pi D_i L_2 (T_{w2} - T_{r2}) \\ \dot{m}_o h_l - \dot{m}_o h_o + \alpha_{i3}\pi D_i L_3 (T_{w3} - T_{r3}) \\ \dot{m}_i - \dot{m}_o \\ \alpha_{i1}\pi D_i (T_{r1} - T_{w1}) + \alpha_o \pi D_o (T_a - T_{w1}) \\ \alpha_{i2}\pi D_i (T_{r2} - T_{w2}) + \alpha_o \pi D_o (T_a - T_{w2}) \\ \alpha_{i3}\pi D_i (T_{r3} - T_{w3}) + \alpha_o \pi D_o (T_a - T_{w3}) \end{bmatrix}$$

and $\mathbf{D}_C$ is the coupling matrix for the condenser states **[5]**.

These 12 state equations represent thermal energy balance of the refrigerate itself and the tubing walls, for each of the 5 distinct heat exchanger regions molded (2 in the evaporator, 3 in the condenser) as well as mass balance of each unit.

STEADY-STATE HEAT EXCHANGER MODEL

Moving from dynamic state equations to a steady state model is easily accomplished by setting the time derivatives to zero. Hence Equations (1) and (2) become Equations (3) and (4), respectively.

$$0 = f_E(x_E, u_E) \qquad (3)$$

$$0 = f_C(x_C, u_C) \qquad (4)$$

For the steady state model, the thermal capacity of the tubing walls, which plays an important role in transient behavior, is

irrelevant. This allows for the grouping of a large number of model parameters into at most 5 overall effective heat transfer coefficients, one for each heat exchanger zone. The derivation of these overall heat transfer equations are shown in the appendix, but as an example, the effective heat transfer per unit length for the superheated phase in the condenser can be seen in Equation (5).

$$U_{c1} = \frac{(\alpha_{ci1}\pi D_{ci} * \alpha_{co}\pi D_o)}{(\alpha_{ci1}\pi D_{ci} + \alpha_{co}\pi D_o)} \quad (5)$$

Since the heat transfer from tube wall to atmosphere is considered as one value this could either encompass fins or other advancements or, just simply, be the heat transfer directly from the coils. Combining all the heat transfer mechanisms into an effective value allows the user to look at the "big picture" and see how the machinery is operating within the various zones.

After adapting the all of the equations shown in He's matrices, the functions to be used in this model are shown in (6) through (10); one equation is given for each refrigerant phase within the heat exchangers.

$$\dot{m}(h_{4'} - h_4) = U_{e1} * l_{e1} * (T_{ea} - T_4) \quad (6)$$

$$\dot{m}(h_1 - h_{4'}) = U_{e2} * l_{e2} * (T_{ea} - T_{er2}) \quad (7)$$

$$\dot{m}(h_2 - h_{2'}) = U_{c1} * l_{c1} * (T_{cr1} - T_{oa}) \quad (8)$$

$$\dot{m}(h_{2'} - h_{2''}) = U_{c2} * l_{c2} * (T_{2'} - T_{oa}) \quad (9)$$

$$\dot{m}(h_{2''} - h_3) = U_{c3} * l_{c3} * (T_{cr3} - T_{oa}) \quad (10)$$

Utilizing a constant effective heat transfer coefficient that incorporates all aspects of heat transfer provides a unique approach to identifying censorious parameters required for an accurate VCC model.

Component Modeling

When looking at the compressor of a VCC as a static component, and assuming that the compressor is well insulated, the relationships between compression and flowrate can be determined utilizing the following equation [5]:

$$\dot{m} = \omega Y_k \frac{1}{v_1}\left[1 + C_k - C_k\left(\frac{P_C}{P_E}\right)^{\frac{1}{2}}\right] \quad (11)$$

Similarly, the operation of the flow restrictor, and its relationship to the changing flowrate, can be determined using (12) adapted from He's research [5]:

$$\dot{m} = C_v A_v \sqrt{\frac{1}{v_3} * (P_C - P_E)} \quad (12)$$

MASS MIGRATION

The dynamic model on which this work is based utilized the mass flow rate as one of the system states. For a steady-state model, the mass flow rate is constant, yet the distribution of refrigerant between the condenser and evaporator changes with the conditions. To incorporate this into our model, the mass of refrigerant in the two heat exchangers is computed and the constraint that the total mass remains constant is enforced.

We simplify the process by assuming that the mass of refrigerant in the system outside the condenser and evaporator is negligible. The mass constraint is shown in equations (13)-(15).

$$\mathrm{M_{total}} = \mathrm{M_{Evaporator}} + \mathrm{M_{Condneser}} \quad (13)$$

where:

$$M_E = \frac{\pi D_{ei}^2}{4}\left[l_{e1}\left(\frac{\bar{\gamma}_E}{v_{4g}} + \frac{1-\bar{\gamma}_E}{v_{4f}}\right) + \frac{l_{e2}}{v_{er2}}\right] \quad (14)$$

$$M_C = \frac{\pi D_{ci}^2}{4}\left[\frac{l_{c1}}{v_{cr1}} + l_{c2}\left(\frac{\bar{\gamma}_C}{v_{2'}} + \frac{1-\bar{\gamma}_C}{v_{2''}}\right) + \frac{l_{c3}}{v_{cr3}}\right] \quad (15)$$

Mean Void Fraction

A mean void fraction (ratio of the volume of vapor to total volume of mixture) is used to help determine the mass of the refrigerant within the two-phase mixture region of the heat exchangers. The mean void fraction is imperative in the use of the lumped parameter method to forecast the transient responses within these heat exchangers. This is important because it relates to the overall system design as well as the control of the system as a whole [10] [11].

Reviewing the previous work done on the mean void fraction and integrating it into this system (13) thru (15) have been determined to reflect the mean void fraction relationships in both the evaporator and the condenser and their contribution to the total mass calculation. These equations were formed applying the Zivi void fraction correlation [10].

PARAMETER DETERMINATION

Equations (6) through (13) comprise 8 nonlinear equations which, when combined with the thermodynamic analysis, predicts system performance as external conditions change (specifically indoor and outdoor temperature). Many of the parameters of the systems (e.g. compressor shaft speed, mass of refrigerant charge) are often found in the manufacturer's literature. Ten of the parameters are less likely to be found, or (like the effective heat transfer characteristics) unique to this modeling effort. These ten are:

- Heat Transfer Coefficient for each Region (U_{e1}, U_{e2}, U_{c1}, U_{c2}, $and\ U_{c3}$)
- Total Length of Tubing within Evaporator (L_E)
- Total Length of Tubing within Condenser (L_C)
- Compressor Displacement (Υ_k)
- Compressor Coefficient (C_k)
- Expansion Valve Coefficient (C_v)

In addition to these model parameters, there are additional variables that are not directly computable from the thermodynamic analysis without already knowing the heat transfer characteristics, namely the lengths of the 5 zones in the evaporator and condenser. Since total lengths of the units are part of the parameter set, there are 3 additional variables that must be solved for each instance of the model.

Using multiple manufacturer's test conditions, we can find parameter (and zone length) values that best fit the published data. Table 2 shows the breakdown on required test conditions compared to the number of unknowns and the number of equations.

Table 2: Relationship Between Number of Test Conditions and Independent Equations

1 Test Condition	13 Unknowns	8 Equations
2 Test Conditions	16 Unknowns	16 Equations
3 Test Conditions	19 Unknowns	24 Equations
4 Test Conditions	21 Unknowns	32 Equations
5 Test Conditions	25 Unknowns	40 Equations

Manufacturers' published test data provide performance data over a range of incoming (indoor) temperature and humidity, coil airflow, and outdoor temperature and humidity. Incoming temperatures range from 70-85° F, and outdoor temps range from 65-115° F in 5 or 10° increments. Table 2 indicates that only two test conditions would be required to uniquely identify the parameters. However, to ensure a robust result, we chose to use roughly 1/3 of the test points to identify the model parameters, the remaining points to validate the model.

Model Demonstration

The process is demonstrated on 3 residential-sized units. We chose 3-ton and 5-ton Goodman units and a 3-ton Bard unit. Test data from 36 separate indoor and outdoor temperatures were obtained and 12 of those were used to identify the parameter values. For each temperature combination, test data were available for a variety of indoor and outdoor humidity levels. We chose the driest conditions used as these best mimics our local climate. The potential complicating factors of high humidity, particularly as it relates to external heat transfer characteristics, is readily acknowledged and discussed in the conclusions of this paper. The variables below are required to be known from the manufacturer's documentation to perform the analysis on the test conditions and utilize the overall model:

- Suction Pressure
- Discharge Pressure
- Indoor Set Point Temperature
- Outdoor Ambient Temperature
- Refrigerant Type
- Compressor Power
- Degrees of Superheat
- Degrees of Subcool
- Compressor Speed
- Flow Restrictor Area (if fixed orifice)
- Charge of System
- Heat Absorption Rate (Refrigeration Load)

The test data provide adequate information to perform a thermodynamic analysis which provides all enthalpy values as well as mass flow rate and heat rejection load for the condenser. This particularly model utilizes R410A, a mixture of refrigerants and hence exhibits glide characteristics (the temperature is not constant in the saturation region). While this is a potentially complicating factor for some mixture-type refrigerants, it is recognized that the maximum glide exhibited by R410A is about 0.5° F and would be responsible for only minor inconsistencies in our model [12]. For mixtures that exhibit larger glides, such as R401A, it is likely that this model would have to be modified to accommodate this characteristic.

RESULTS

Parameter Identification

Table 2 shows the results of the parameter identification process for the three units. The parameters were identified using the "solver" add-in in Microsoft Excel®.

Table 3 shows the residuals from the parameter identification process. After the thermodynamic analysis, the model equations are somewhat de-coupled allowing us to segment the process into three different sheets dealing with the evaporator, the condenser and the entire system. The residuals were computed as an average of the percent error over the 12 test conditions.

Table 2: Parameter identification results

	Goodman 3 Ton Unit	Goodman 5 Ton Unit	Bard 3 Ton Unit
L_E $[ft]$	102.81	176.1	149.2
U_{e1} $\left[\frac{BTU}{hr*ft*F}\right]$	8.0751	7.742	7.48
U_{e2} $\left[\frac{BTU}{hr*ft*F}\right]$	3.2317	2.943	1.798
L_C $[ft]$	92.59	150.9	158.9
U_{c1} $\left[\frac{BTU}{hr*ft*F}\right]$	19.704	31.788	3.305
U_{c2} $\left[\frac{BTU}{hr*ft*F}\right]$	40.3034	38.004	29.016
U_{c3} $\left[\frac{BTU}{hr*ft*F}\right]$	23.3156	19.087	4.391
V_k $[ft^3]$	0.0004	0.00074	0.0004
C_k	0.3410	0.43535	0.4085
C_v	0.6719	0.5928	0.593

Table 3: Residuals from Parameter Identification

	$\dot{Q}_L$ Residual	$\dot{Q}_H$ Residual	$\dot{m}$ Residual
Goodman 3 Ton Unit	2.9%	2.8%	3.5%
Goodman 5 Ton Unit	1.5%	1.5%	1.2%
Bard 3 Ton Unit	2.4%	2.4%	2.4%

Model Validation

Figure 4 shows a map of the combinations of indoor and outdoor temperatures used to identify the parameters and validate the model.

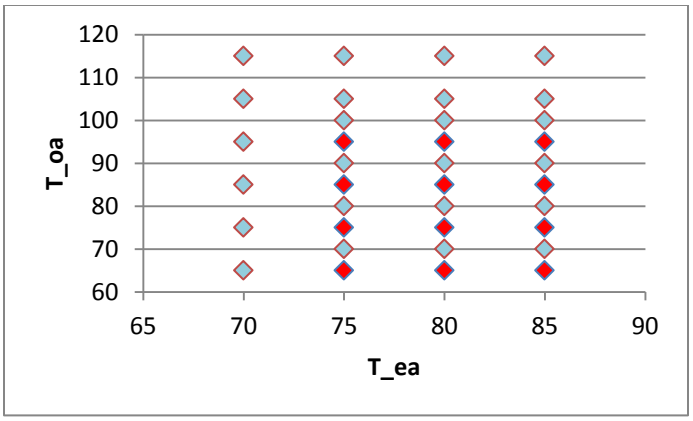

Figure 4: Map of test conditions used for parameter identification (red) and model validation (grey). The axes are outside air temp (°F, vertical axis) and evaporator air temp (°F, horizontal axis).

As shown, test conditions both within and outside the region spanned by the parameter identification process were used to validate the model. As a measure of model fidelity, the error in predicting cooling load was used. The results are shown in Table 4 below.

Table 4: Model Errors

Model	$\dot{Q}_L$ Average Error
Goodman 3 Ton Unit	3.7%
Goodman 5 Ton Unit	2.0%
Bard 3 Ton Unit	2.3%

DISCUSSION

The parameter identification process results in physically reasonable parameter values. For example, the overall heat transfer characteristics in the internally wetted regions of the coils (region 2 of the condenser and region 1 of the evaporator) are considerably higher than those of the superheat regions, as would be predicted by theory. In addition, the heat transfer parameters within the saturated regions are relative consistent from unit to unit. This would also be expected if all units used similar coil designs of round tubes with external fins. Comparing the 3-ton and 5-ton Goodman units, we find that the overall coil lengths track the unit capacity well. The 5-ton unit has 67% more capacity compared to the 3 ton unit while the evaporator coil is 70% longer. The differences for the 3-ton unit from the 2nd manufacturer are more difficult to explain but could be due to fundamental differences in system design. For

example, the Goodman units use fixed orifice expanders while the Bard unit utilizes a TEX.

CONCLUSION

This paper addresses one of the barriers in developing and using VCC performance models, namely, the identification of parameter values required to make these models useful. A significant innovation of the approach presented here is the development of an overall effective heat transfer coefficient for each region of the heat exchangers, combing the internal convection, tube wall conduction and external convection and fin geometry into a single parameter the value of which is developed from published test condition. Model validation was performed using test conditions that spanned and exceeded the range of conditions used for parameter identification. Results of the modeling and validation process showed model errors averaging less than 4% through the range of available data.

To make this approach more broadly applicable, several modifications and additions are envisioned. The increasing popularity of zeotropic refrigerants (i.e. mixtures) dictates that the model should be modified (or minimally validated) for those refrigerants that exhibit significant glide characteristics. Also, the role of higher humidity environments, particularly for indoor air conditions that lead to high condensation rates on the evaporator coils will have to be further investigated as that will likely lead to modifications in the overall heat transfer coefficients.

Finally, it is anticipated that this process of identification can be used to inform the development and application of dynamic models and simulations that can better inform control and fault detection applications.

NOMENCLATURE

Symbols

A	Area $[ft^2]$
D	Diameter $[ft]$
h	Refrigerant Enthalpy $\left[\frac{BTU}{lbm}\right]$
L	Total Length $[ft]$
l	Zone Length $[ft]$
M	Mass $[lbm]$
$\dot{m}$	Flowrate $\left[\frac{lbm}{hr}\right]$
P	Refrigerant Pressure $\left[\frac{lbf}{in^2}\right]$
$\dot{Q}$	Heat Transfer Rate $\left[\frac{BTU}{hr}\right]$
s	Refrigerant Entropy $\left[\frac{BTU}{lbm*R}\right]$
T	Temperature $[F]$
U	Effective Heat Transfer coeff $\left[\frac{BTU}{hr*ft*F}\right]$
$\dot{W}$	Work $\left[\frac{BTU}{hr}\right]$
x	Refrigerant Quality $[dimensionless]$
α	Convective Heat Transfer coeff $\left[\frac{BTU}{hr*F}\right]$
$\bar{\gamma}$	Mean Void Fraction $[dimensionless]$
ν	Refrigerant Specific Volume $\left[\frac{ft^3}{lbm}\right]$
ρ	Refrigerant Density $\left[\frac{lbm}{ft^3}\right]$

Subscripts

$2, 2', 2'', 3$	Zone Numbers for Condenser
$4, 4', 1$	Zone Numbers for Evaporator
$4f$	Saturated Fluid at State 4
$4g$	Saturated Vapor at State 4
C	Condenser
$c1, c2, c3$	Zones in Condenser
ci	Inner Tube of Condenser
co	Condenser Tubing to Ambient Air
$cr1, cr3$	Average Values of Zones in Condenser
$cw1$	Average Wall Value in Condenser Zone
E	Evaporator
$e1, e2$	Zones in Evaporator
ea	Temperature of Conditioned Space
$er2$	Average Values in Zone of Evaporator
ei	Inner Tube of Evaporator
f	fluid (liquid) phase
g	vapor (gas) phase
H	Total Heat Rejected at the Condenser
i	inner (diameter)
in	Input
L	Total Heat Absorbed at the Evaporator
o	Outer (diameter)
oa	Outside Air (Temperature)
s	Entropy
sat	Two-Phase Zone
SH	Superheat Region
sub	Subcool Region
w	wall (of condenser or evaporator)

ACKNOWLEDGMENTS

The authors gratefully acknowledge the support of the US Department of Energy Industrial Assessment Center program (EERE-AMO) and the support of the Department of Mechanical and Biomedical Engineering at Boise State University.

REFERENCES

[1] Y. A. Cengel and M. A. Boles, Thermodynamics: An Engineering Approach, Sixth Edition, New York, NY: McGraw-Hill Companies, 2008.

[2] G. Davis and T. Scott, "Component Modeling Requirements for Refrigeration System Simulation," in *International Compressor Engineering Conferences*, West Lafayette, Indiana, 1976.

[3] J. Chi and D. Didion, "A Simulation Model of the Transeient Performance of a Heat Pump," *International Journal of Refrigeration*, vol. 5, no. 3, pp. 176-184, 1982.

[4] M. de Lemos and E. Zaparoli, "Steady-State Numerical Solution of Vapor Compression Refrigeration Units," in *International Refrigeration and Air Conditioning Conference*, West Lafayette, Indiana, 1996.

[5] X.-D. He, "Dynamic Modeling and Mulitvariable Control of Vapor Compression Cycles in Air Conditioning Systems," Massachusetts Institute of Technology, Cambridge, Massachusetts, 1996.

[6] B. Li and A. G. Alleyne, "A Dynamic Model of a Vapor Compression Cycle with Shut-Down and Start-Up Operations," *International Journal of Refrigeration*, pp. 538 - 552, 2010.

[7] T. L. McKinley and A. G. Alleyne, "An Advanced Nonlinear Switched Heat Exchanger Model for Vapor Compression Cycles Using the Moving-Boundary Method," *International Journal of Refrigeration*, pp. 1254 - 1264, 2008.

[8] S. Bendapudi, "Development and Evaluation of Modeling Approaches for Transients in Centrifugal Chillers," Purdue University, West Lafayette, IN, 2004.

[9] H. Qiao, V. Aute and R. Radermacher, "An Improved Moving Boundary Heat Exchanger Model with Pressue Drop," in *International Refrigeration and Air Conditioning Conference*, 2014.

[10] B. B. B. B. G.L. Wedekind, "A System Mean Void Fraction Model for Predicting Various Transient Phenomena Associated With Two-Phase Evaporating and Condensing Flows," *International Journal of Multiphase Flow*, pp. 97 - 114, 1976.

[11] B. Beck and G. Wedekind, "A Generalization of the System Mean Void Fraction Model for Transient Two-Phase Evaporating Flows," *ASME*, pp. 81 - 85, 1981.

[12] E.I. du Pont and de Nemours and Company, "Thermodynamic Propoerites of DuPont TM Suva (r) 410A Refrigerant," E.I. du Pont De Nemours and Company , Wilmington, DE, 2004.

APPENDIX

EFFECTIVE HEAT TRANSFER DERIVATION

The purpose of the moving boundary method is to divide the heat exchangers into various control volumes based off of the particular refrigerant phase. In the case of the condenser these flow characteristics that make up the phases include the superheated vapor, the two-phase flow and the subcooled liquid. In the case of the evaporator the flow characteristics include the two-phase flow and the superheated vapor.

The main difference between He's work and the development described in this paper is the use of heat transfer values. This paper reflects an effective heat transfer value as opposed values computed strictly from the geometry. Below is the derivation process used for each of the equations for the boundary phases, the specific one derived below is for the superheated phase within the condenser. All of the "original" equations are directly from He's dissertation for his PhD in Mechanical Engineering and the "modified" equations are the modified equations that utilize the nomenclature used throughout this paper [5].

$$\alpha_{i1}\pi D_i(T_{r1} - T_{w1}) + \alpha_o\pi D_o(T_a - T_{w1}) = 0 \quad \text{(A-1)}$$

$$\alpha_{ci1}\pi D_{ci}(T_{cr1} - T_{cw1}) + \alpha_{co}\pi D_o(T_{oa} - T_{cw1}) = 0 \quad \text{(A-2)}$$

$$\dot{m}_i h_i - \dot{m}_i h_g + \alpha_{i1}\pi D_i L_1(T_{w1} - T_{r1}) = 0 \quad \text{(A-3)}$$

$$\dot{m}(h_2 - h_{2,}) + \alpha_{ci1}\pi D_{ci} l_{c1}(T_{cw1} - T_{cr1}) = 0 \quad \text{(A-4)}$$

In order to eliminate the wall temperature to gain an effective heat transfer T_{cw1} from (A-4) must be solved for, as shown.

$$T_{cw1} = T_{cr1} - \frac{\dot{m}(h_2 - h_{2,})}{\alpha_{ci1}\pi D_{ci} l_{c1}} \quad \text{(A-5)}$$

At this point there is the matter of substituting (A-5) in (A-2):

$$\alpha_{ci1}\pi D_{ci}\left(T_{cr1} - \left[T_{cr1} - \frac{\dot{m}(h_2 - h_{2,})}{\alpha_{ci1}\pi D_{ci} l_{c1}}\right]\right) + \alpha_{co}\pi D_o\left(T_{oa} - \left[T_{cr1} - \frac{\dot{m}(h_2 - h_{2,})}{\alpha_{ci1}\pi D_{ci} l_{c1}}\right]\right) = 0 \quad \text{(A-6)}$$

Simplifying:

$$\dot{m}(h_2 - h_{2,}) + \frac{\alpha_{ci1}\pi D_{ci}*\alpha_{co}\pi D_o}{\alpha_{ci1}\pi D_{ci}+\alpha_{co}\pi D_o} * l_{c1} * (T_{oa} - T_{cr1}) = 0 \quad \text{(A-7)}$$

$$Let\ U_{c1} = \frac{(\alpha_{ci1}\pi D_{ci}*\alpha_{co}\pi D_o)}{(\alpha_{ci1}\pi D_{ci}+\alpha_{co}\pi D_o)}$$

$$\dot{m}(h_2 - h_{2,}) = l_{c1} * U_{c1} * (T_{cr1} - T_{oa}) \quad \text{(A-8)}$$

Once simplified the equation (A-8) knowing that U_{c1} is to be considered the effective heat transfer per unit length. The remaining derived equations for the boundary lengths at the condenser and the evaporator follow this form, but for the sake of brevity are not shown.